**Academic Journal of Science and Technology**
ISSN: 2771-3032 | Vol. 9, No. 3, 2024

# Experimental Research on Impact Resistance Test of Polycrystalline Diamond Compact Based on Digital Image Correlation Method

**Yuanjing Zhao, Jian Shi*, Xinfeng Xu**

School of Mechanical Engineering, Southwest Petroleum University, Chendu 610500, China
* Corresponding author

**Abstract:** In this study, the impact resistance of Polycrystalline Diamond Compact (PDC) was studied with DIT drop weight tester and high speed camera. The surface of PDC was analyzed by Digital Image Correlation (DIC). The reason of impact failure of PDC was obtained by using the surface strain field of PDC. The results show that local delamination occurs near the impact point of the polycrystalline layer. The brittle fracture occurs at the maximum tensile strain of the impact resistant composite sheet. The quantitative relationship between the surface strain and the image obtained by DIC can effectively reflect the whole process of PDC composite failure, and can reasonably explain the failure process of PDC composite, and provide scientific research methods for engineering applications.

**Keywords:** Digital Image Correlation; Polycrystalline Diamond Compact; Impact resistance; Strain.

PDC is the abbreviation of polycrystalline diamond composite sheet, and its production process is sintered by diamond powder (0.5-2.5 mm) on a cemented carbide substrate at high temperature and high pressure (1,300-1,500 ℃, 5-7 GPa).

## 1. Introduce

PDC composite sheet is short for polycrystalline diamond composite sheet. Its production process is sintered from diamond powder (0.5-2.5mm) on cemented carbide matrix at high temperature and high pressure (1 300-1 500 ℃, 5-7 GPa) [1]. At present, there are three experimental methods used to study the impact resistance of PDC composite sheets at home and abroad [2]. The rotary impact method of PDC turning grooved granite is to make PDC composite sheets into cemented carbide tools, cut granite according to a certain cutting speed and feed speed, and take the number of impact times required for granite defects as the evaluation standard. Because granite is an anisotropic material, the reliability of the measured data is not high. High-speed moving particle erosion method is to accelerate the projectile particles to form an impact current, which erodes the surface of PDC composite sheet. Finally, the impact resistance of PDC composite sheet is comprehensively evaluated according to factors such as the quality of PDC composite sheet, the material and speed of erosive particle before and after erosion. This experimental process and analysis method are relatively complex and require high requirements for experimental equipment. So it is rarely used in practical application; The heavy block impact method is carried out on the impact frame of the suspended wire. It takes the total impact work required for the specimen to be destroyed as the evaluation standard, and this method ignores the failure form in the actual working condition of the PDC composite.

. FuXiao Zhang[1] conducted experiments on PDC of five different diamond particles and analyzed their fracture morphology through scanning electron microscope. Finally, he concluded that the finer the diamond particles and the coarser the WC particles, the better the impact resistance of PDC. Xi[2] established a numerical model for cutting hard rock with a monomeric polycrystalline diamond composite (PDC) bit, and analyzed the effects of amplitude, frequency, time parameters and waveform on the penetration depth of PDC bit during torsional impact drilling. The results show that the numerical simulation results are in good agreement with the laboratory test results, and the correctness of the method is verified. Zhiling Xiao[3] analyzed the equal effect, impact force and crack growth of polycrystalline layer of conical PDC teeth with diameter D30 series by ABAQUS. The final result is that the series can withstand up to 7500J of impact work, and the failure mode of the conical teeth includes the ring loss at the top of the PDC layer, the transverse spalling of the PDC layer and the overall cracking of the conical teeth.

Li[4] studied the performance of polycrystalline diamond compact PDC tools against different static thrust, impact and cutting loads on Missouri red granite and Halston Limestone by using drop hammer and linear cutting impact table. The results show that the combined mode of cutting shocks is very effective in very hard rocks. wang[5] et al. used a drop hammer impact testing machine with loaded high-cycle fatigue mode, and considered the effects of impact energy, ball surface area, cemented carbide matrix thickness and PCD layer thickness on the impact resistance of PDC. The results show that the greater the impact force, the higher the crushing rate; When the impact force is the same, the larger the surface area of the ball, the lower the crushing rate. When the impact force is the same, the larger the surface area of the ball, the lower the crushing rate; The greater the thickness of the WC-Co tungsten carbide tooth matrix and the smaller the thickness of the PCD layer, the better the impact resistance of the spherical tooth.

Zhang Suhui et al. [7] explored the performance changes of PDC composites at different temperatures. The results show that the performance of PDC decreases with the increase of temperature, especially when the PDC reaches 800 ℃. At the same time, it is suggested that using PDC with different performance in different parts of the bit can effectively

improve the life of PDC bit. Sun Wei et al. [8] used scanning electron microscopy and PDC dynamic load resistance tester to conduct comparative experiments on filled and unfilled diamond composite sheets. The results show that the total impact energy of the filled diamond composite can reach 450 J.

Digital image correlation is a more mature non-contact measurement method, which is based on the artificial or natural scattering changes before and after the deformation of the object, so as to extract the full-field displacement and deformation information.

Many scholars in the international arena have used the DIC technique for strain measurements on a wide range of materials. Xianyin Qi et al [9] obtained the full-field displacement evolution law of the complete loading process of composite rock by DIC. The final characteristics expressed by each displacement cloud map fit with the damage characteristics of the specimen. Tung et al [10] performed tensile tests on steel specimens and showed that the modulus of elasticity measured by strain gauges was 206 GPa, and the modulus of elasticity of steel specimens determined by DIC technique was equal to 201 GPa. A.J et al. [11] successfully generated the full in-plane strain and out-of-plane deformation data of the single lap joint of prepreg and non-compensed fabric composite materials through DIC, and determined the specific position and magnitude of the maximum principal strain.

Sudarsanan et al. [12] analyzed the surface of an asphalt concrete beam under fatigue loading by DIC technology and obtained that the maximum vertical strain (εyy) of the beam was only 5% at 10℃ and increased to 25% at 30 ℃. Liu et al. [13] quantified the micron-scale in-plane plastic strain through DIC, and finally analyzed that the maximum surface strain was independent of the indentation depth. Many research results show that DIC technology is suitable for full-field strain measurement of a variety of materials under different loading modes, but there are few relevant studies and data on impact resistance of PDC composites using DIC technology.

The drop weight experiment method adopted in this paper is to use DIT drop weight testing machine and high-speed camera to collect the load of the drop weight impact process and the image of PDC surface. DIC method was used to analyze the strain field on the surface of PDC composite sheet, and the impact work value required by crack and delamination on the specimen surface was used as the index to evaluate the impact resistance of PDC composite sheet.

## 2. PDC Impact Test

PDC composite sheets are two kinds of anti-impact and anti-wear composite sheets provided by a Chinese manufacturer, and their basic dimensions are shown in Figure 1. Before the test, the surface of PDC sample was sprayed with speckle, as shown in Figure 2.

The testing machine adopts the DIT drop weight testing machine with the maximum impact power of 300J. During the test, the force signal of the whole impact process was collected by the ut36 dynamic signal acquisition device connected to the sensor of the hammer head of the drop weight testing machine, and the acquisition frequency was 2.048MHz. The high-speed camera is NAC HX-6, with a frame rate of 50000FPS and a pixel of 320×168 pixels. Halogen lamp cold light source was used to irradiate the surface of PDC sample for light intensity compensation, and the test device was shown in Figure 2.

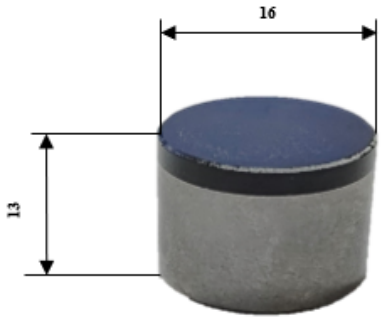


**Figure 1.** Basic size of PDC

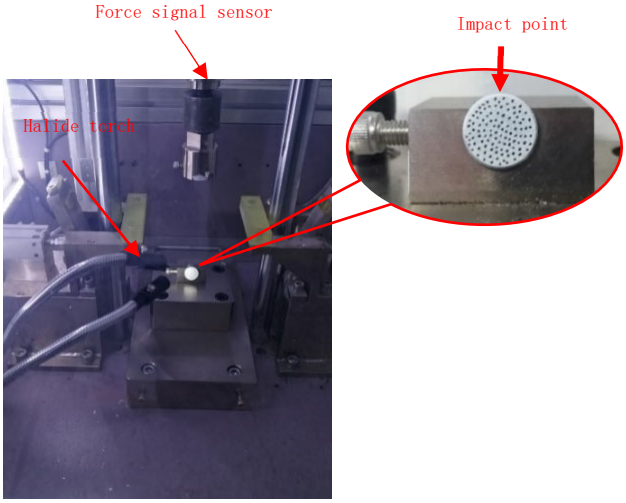


**Figure 2** Test device

Since there is no unified test standard, the impact loading scheme for the impact resistance of PDC composite sheet is studied. The loading process is divided into three steps. The first step adopts 30 J impact power for 10 times, the second step adopts 50 J impact power for 10 times, and the third step adopts 80 J impact power for 10 times. Once the PDC composite is cracked, the test is stopped.

As a non-contact deformation measurement technology, when the surface of the sample is deformed, the gray level of the surface image will change. The NCORR-DIC module calculates the mapping relationship between the gray level changes of the observation points before and after the deformation (the mapping relationship is called the displacement shape function [15]-[18]).

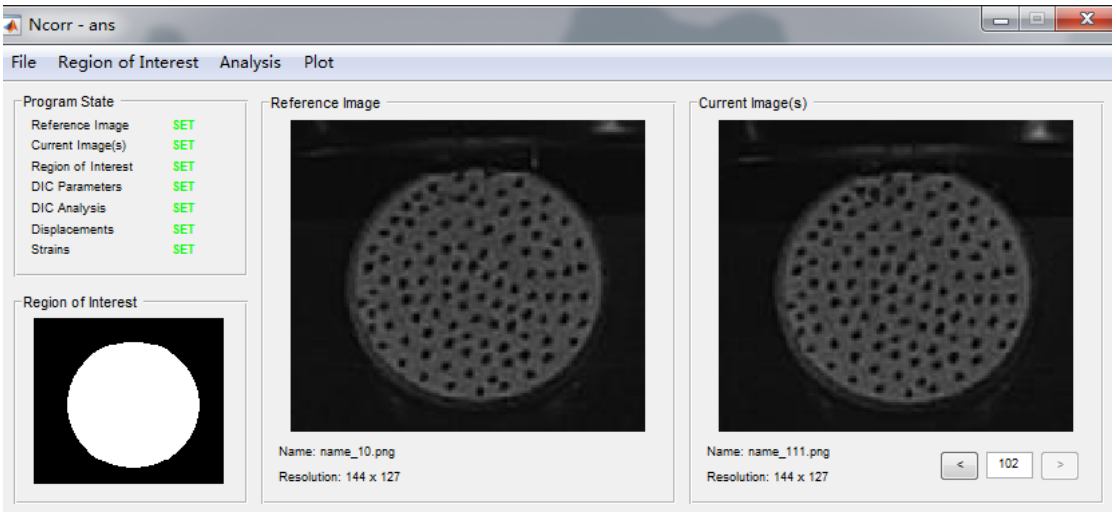


**Figure 3.** Ncorr module interface

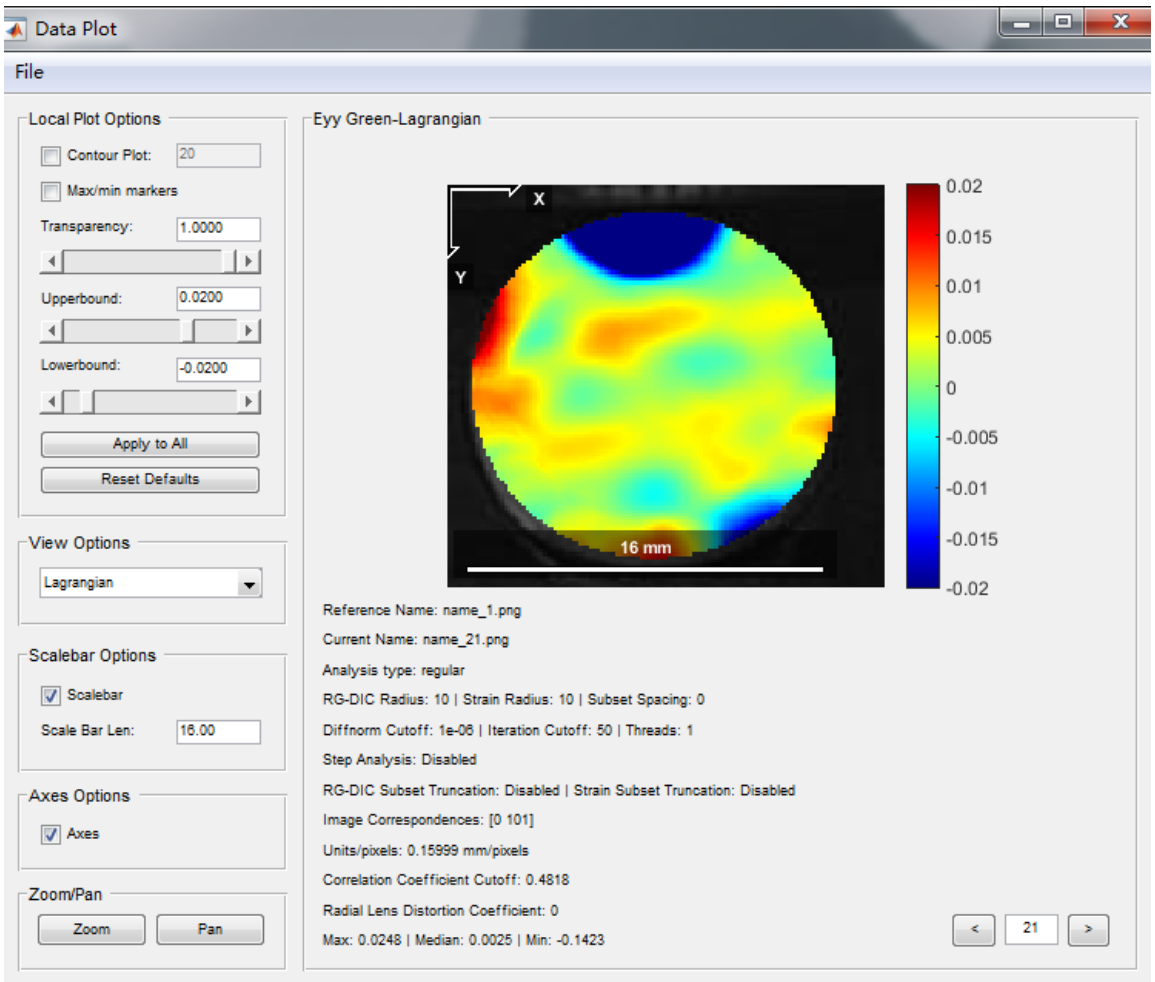


**Figure 4.** Plot module interface

After the displacement shape function is obtained, the strain is calculated from the displacement gradient, as shown in Figure 3. The first frame picture and the subsequent frame picture are used as the reference object and the calculation object respectively. The Resolution of Interest (ROI) is set as the entire PDC surface area (145 pixel×145 pixel), and the

sub-areas are sown according to the seeds of (10 pixel×10 pixel). The strain cloud map required for later analysis is exported in the Plot module, as shown in Figure 4.

# 3. Results and Discussion

## 3.1. Impact Load

The specific test procedure and failure information are shown in Table 1, and the load time curve is shown in Fig. 5.

**Table 1.** Impact process and failure forms of specimens

| | Type | 30J(Impact number of times ) | 50J(Impact number of times ) | 80J(Impact number of times) | failure mode |
|---|---|---|---|---|---|
| #1 | impact resistance | 10 | 10 | 1 | PCD crush |
| #2 | impact resistance | 10 | 10 | 1 | PCD crush |
| #3 | Wear resistance | 7 | 0 | 0 | PCD delamination |
| #4 | Wear resistance | 10 | 7 | 0 | PCD delamination |

From the load time curve, it can be seen that when the impact work is 30 J, the impact load is about 55 kN; when the impact work is 50 J, the impact load of specimen #1, #2 and #4 is about 80 kN, and that of specimen #3 is about 65 kN. The results show that: with the increase of impact power, the maximum impact load also increases; impact power of 80 J, the corresponding impact load when the specimen crumbles is smaller than the impact load of 30 J and 50 J, indicating that the specimen has internal defects due to multiple impacts, and the failure load is smaller.

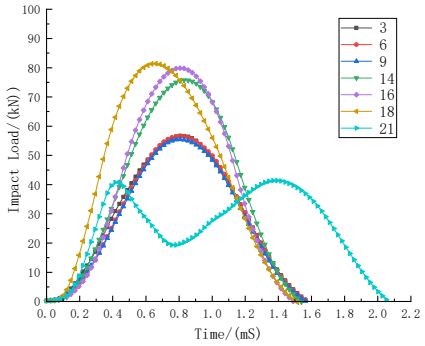


(a) # 1 test specimen

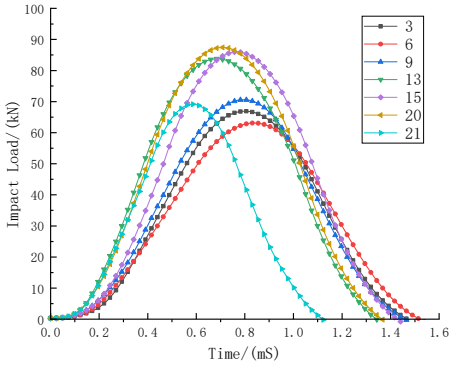


(b) # 1 test specimen

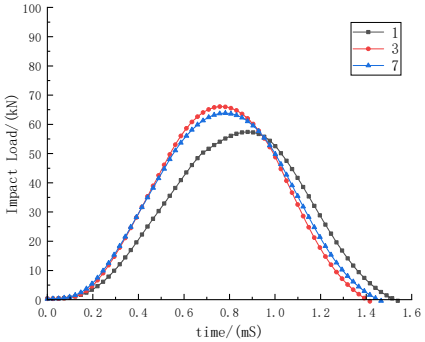


(c) # 1 test specimen

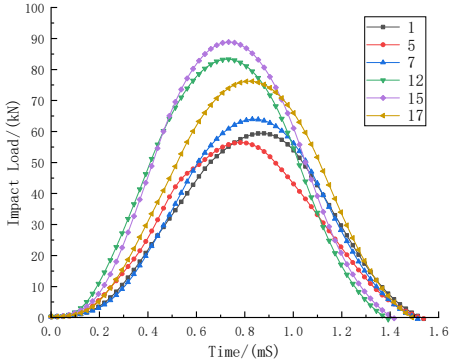


(d) # 2 test specimen

**Figure 5.** Load-time curve of each specimen

## 3.2. Strain analysis

Figure 6 shows the strain cloud diagram of the surface of PDC composite sheet during the impact of specimen #1. The results show that when the impact work is 30 J, the surface of the PDC composite piece locally has a large strain (the moment of maximum load); There is basically no residual strain generation on the surface after impact (at the moment when the load is zero), indicating that the PDC composite sheet is predominantly elastically deformed under the impact load. With the increase of the number of impacts, the strain concentration area and the maximum strain are basically unchanged, indicating that the PDC composite sheet basically has no residual strain under the action of lower impact power. When the impact power is 50 J, the local strain value is larger than the impact process of 30 J, and the strain concentration area is also more than the impact process of 30 J. The strain

concentration area is also more than the impact process of 30 J;

After several impacts, there are residual strains generated on the surface of the PDC composite sheet. When the impact power is 80 J, after an impact, PDC composite sheet crumbles, before crumbling, the maximum strain on the surface of the PDC composite sheet and the strain concentration area are larger than the impact process of 30 J and 50 J, and the traces of the crumbling are basically consistent with the traces of the residual strain appearing at the time of the 50 J impact, indicating that in the process of multiple impacts with an impact power of 50 J, the residual strain on the surface of the PDC composite sheet results in the destruction of the PDC composite sheet. composite sheet destruction.

Fig. 7 shows the strain cloud diagram of the surface of PDC composite sheet under different impact work of specimen #2. Comparing with specimen #1, the results show that although the strains in the edge region of the surface of the PDC composite sheet are different in the process of impact loading, the regions of surface strain distribution and the maximum strain values are basically the same in the impact process. In particular, the damage forms of the PDC composite sheets are basically the same, i.e., chipping produced by crushing at the top and cracking in the vertical direction.

Fig. 8 and Fig. 9 show the strain cloud diagrams of specimens #3 and #4 in the impact process, respectively. Comparison with Fig. 6 and Fig. 7 shows that when specimen #3 is impacted at 30 J, the maximum value of strain on the surface of the PDC composite sheet and the strain distribution are basically the same as that of specimens #1 and #2; with the increase in the number of impacts, the position in contact with the hammer head has a larger value of strain and a larger strain occurs there, which leads to delamination of the polycrystalline layer of PDC composite sheet. #4 specimen in 50 J impact, the same as #3 specimen, and the hammer head contact position PDC composite sheet polycrystalline layer delamination.

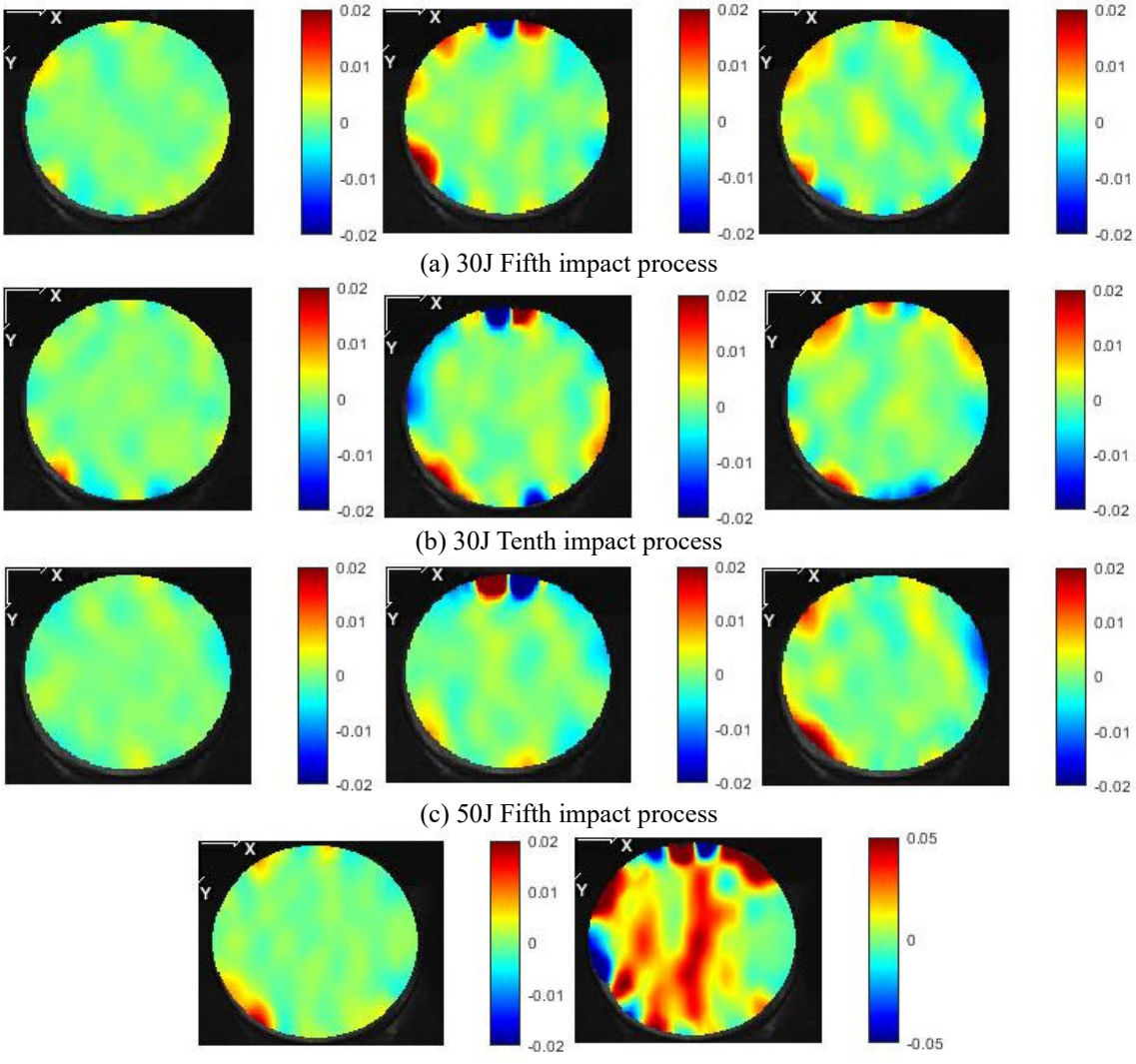


(a) 30J Fifth impact process

(b) 30J Tenth impact process

(c) 50J Fifth impact process

(d) 80J first impact process

**Figure 6.** Strain cloud diagram of #1 specimen failure process

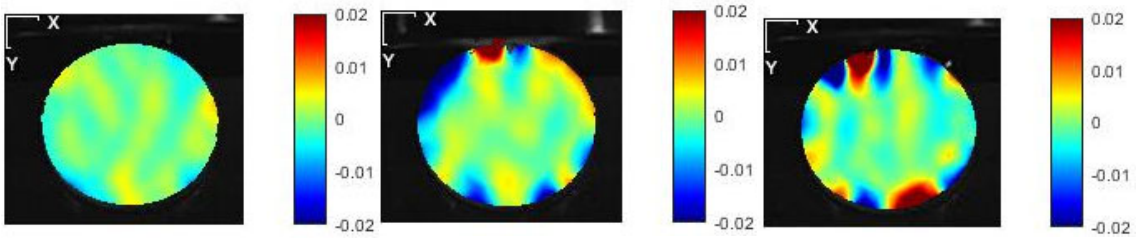


(a) 30J Fifth impact process

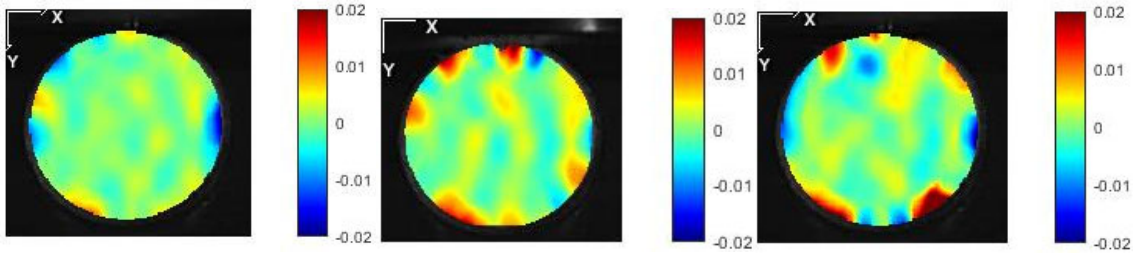


(b) 30J Tenth impact process

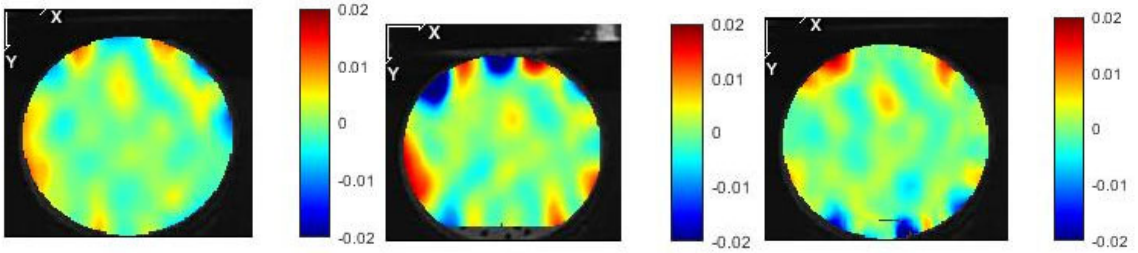


(c) 50J Fifth impact process

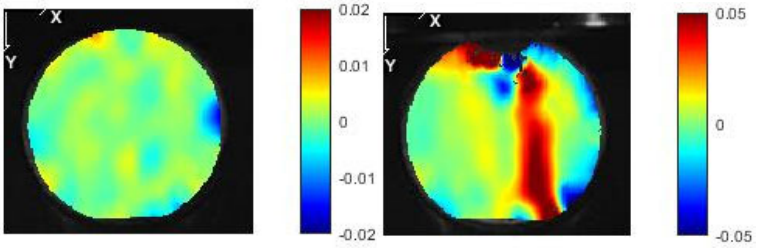


(d) 80J first impact process

**Figure 7.** Strain cloud diagram of #2 specimen failure process

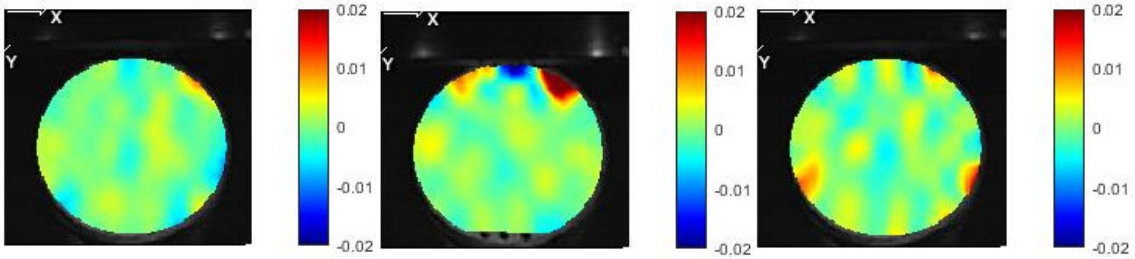


(a) 30J Fifth impact process

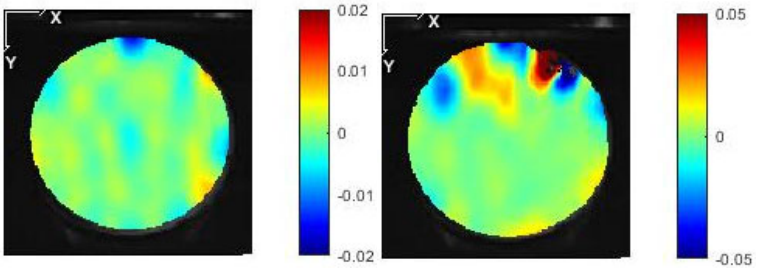


(b) 30J Seventh impact process

**Figure 8.** Strain cloud diagram of #3 specimen failure process

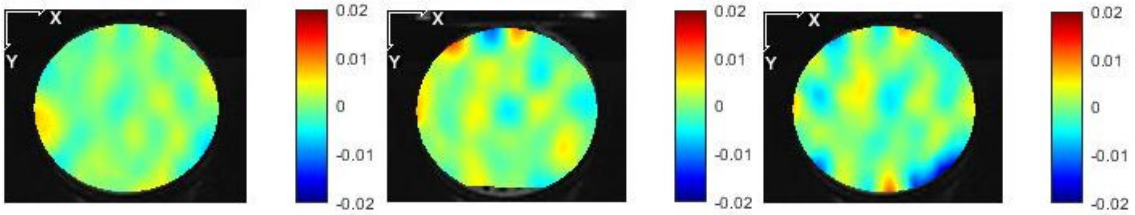


(a) 30J Fifth impact process

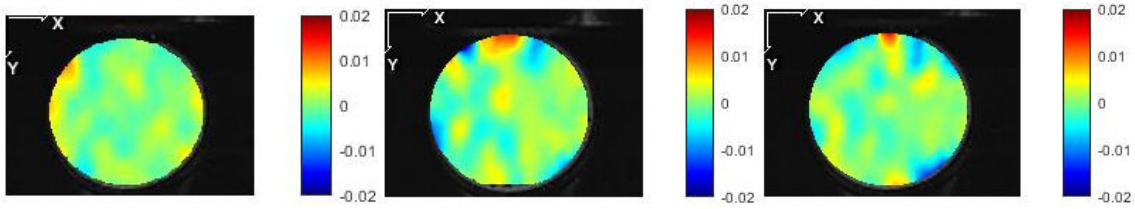


(b) 30J Tenth impact process

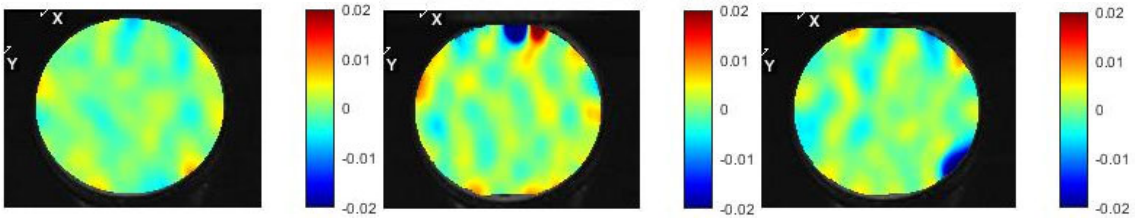


(c) 50J Fifth impact process

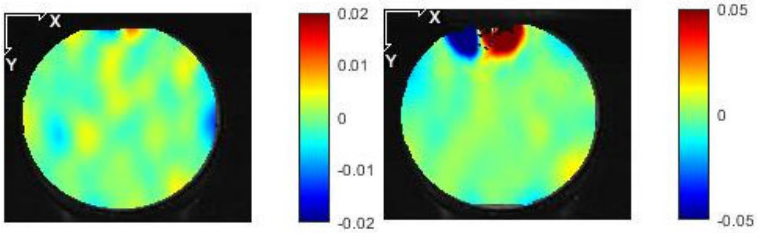


(d) 50J Seventh impact process

**Figure 9.** Strain cloud diagram of #4 specimen failure process

Figure 10 for the PDC composite piece impact force analysis model. Because the thickness of the polycrystalline layer on the PDC composite sheet is much smaller than the height of the base, the polycrystalline layer is subjected to stress according to the plane stress analysis; at the same time, the PDC composite sheet is mounted in a fixed fixture, and the acceleration generated by the falling hammer test is negligible, so the stress analysis of the PDC composite sheet is analyzed using the elastic mechanics in the close solution, where $\alpha = \pi$, $\beta = 0$ and then get the circumferential stress component.

$$\begin{cases} \sigma_\rho = -\dfrac{2F}{\pi}\dfrac{\cos\varphi}{\rho} \\ \sigma_\varphi = 0 \\ \tau_{\rho\varphi} = \tau_{\varphi\rho} = 0 \end{cases} \tag{1}$$

In Eq. (1): $\sigma_\rho$ , $\sigma_\varphi$ , $\tau_{\rho\varphi}$ and $\tau_{\varphi\rho}$ are the radial, circumferential stress and shear stresses of the PDC respectively.

Substituting the stress components into the physical equations, each of the strain components can be obtained

$$\begin{cases} \varepsilon_\rho = -\dfrac{2F\left(1-\mu^2\right)}{\pi E}\dfrac{\cos\varphi}{\rho} \\ \varepsilon_\varphi = \dfrac{2\mu F\left(1+\mu\right)}{\pi E}\dfrac{\cos\varphi}{\rho} \\ \gamma_{\rho\varphi} = 0 \end{cases} \tag{2}$$

In formula (2) $\varepsilon_\rho$ , $\varepsilon_\varphi$ , $\gamma_{\rho\varphi}$ and are the radial strain, circumferential strain and shear strain of PDC composite sheet respectively. $E$ is the elastic modulus and $\mu$ is Poisson's ratio.

In order to compare with the results obtained by NCORR, the strain component under cartesian coordinates can be obtained by changing the polar coordinates in equation (2) to cartesian coordinates. During calculation, the elastic modulus $E$ of PDC composite sheet is 860 GPa, Poisson's ratio $\mu$ is 0.07, and the maximum impact load is F. The theoretical calculation is compared with the strain actually calculated by Ncorr module, and the results are shown in Table 2.

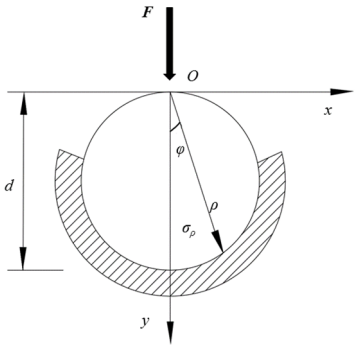


**Figure 10.** Simplified mechanical model

$$\begin{cases} \varepsilon_x = \dfrac{2F\left(1-\mu^2\right)}{\pi E}\dfrac{yx^2}{\left(x^2+y^2\right)^2} + \dfrac{\mu}{1-\mu}\dfrac{y^3}{\left(x^2+y^2\right)^2} \\ \varepsilon_y = -\dfrac{2F\left(1-\mu^2\right)}{\pi E}\dfrac{y^3}{\left(x^2+y^2\right)^2} + \dfrac{\mu}{1-\mu}\dfrac{yx^2}{\left(x^2+y^2\right)^2} \\ \gamma_{xy} = -\dfrac{4(1+\mu)F}{\pi E}\dfrac{y^2x}{\left(x^2+y^2\right)^2} \end{cases} \quad (3)$$

**Table 2.** Comparison between theoretical calculation and NCORR calculation results

| | precalculated position(x,y) | F/kN | $\varepsilon_x$ | $\varepsilon_{xDIC}$ | absolute error | $\varepsilon_y$ | $\varepsilon_{yDIC}$ | absolute error |
|---|---|---|---|---|---|---|---|---|
| #1-5 | (-15,39) | 57.24 | 0.13% | 0.12% | 8.27% | -0.59% | -0.53% | 10.57% |
| | (30,88) | 57.24 | 0.05% | 0.05% | 4.95% | -0.28% | -0.24% | 13.40% |
| #1-9 | (-19.22) | 55.49 | 0.33% | 0.30% | 10.10% | -0.43% | -0.40% | 6.80% |
| | (4,47) | 55.49 | 0.05% | 0.05% | 6.03% | -0.57% | -0.55% | 3.82% |
| #1-15 | (-36,69) | 79.89 | 0.12% | 0.14% | 14.69% | -0.36% | -0.38% | 6.00% |
| | (-11,9) | 79.89 | 1.06% | 1.10% | 4.05% | -0.84% | -0.76 | 9.95% |
| #2-5 | (-10,13) | 71.49 | 0.66% | 0.61% | 8.02% | -1.04% | -1.03% | 0.83% |
| | (14,36) | 71.49 | 0.16% | 0.17% | 9.35% | -0.69% | -0.68% | 2.04% |
| #2-10 | (-24,18) | 68.88 | 0.48% | 0.49% | 2.56% | -0.29% | -0.29% | 0.80% |
| | (15,10) | 68.88 | 0.79% | 0.78% | 1.06% | -0.40% | -0.45% | 13.51% |
| #2-15 | (24,16) | 85.99 | 0.64% | 0.62% | 3.54% | -0.32% | -0.35% | 8.28% |
| | (45,76) | 85.99 | 0.14% | 0.14% | 2.44% | -0.35% | -0.34% | 1.69% |
| #2-20 | (-5,20) | 87.45 | 0.28% | 0.32% | 13.57% | -2.05% | -1.99% | 3.16% |
| | (32,36) | 87.45 | 0.35% | 0.34% | 1.85% | -0.42% | -0.40% | 5.68% |
| #3-5 | (20,16) | 72.45 | 0.56% | 0.55% | 1.56% | -0.38% | -0.43% | 12.78% |
| | (-17,15) | 72.45 | 0.62% | 0.56% | 10.05% | -0.50% | -0.54% | 7.54% |
| #4-5 | (-8,20) | 69.41 | 0.31% | 0.37% | 19.69% | -1.33% | -0.60% | 54.88% |
| | (-9,17) | 69.41 | 0.45% | 0.42% | 6.91% | -1.30% | -0.54% | 58.33% |
| #4-10 | (-40,78) | 69.26 | 0.10% | 0.13% | 32.99% | -0.29% | -0.30% | 1.80% |
| | (-35,32) | 69.26 | 0.30% | 0.29% | 2.09% | -0.25% | -0.22% | 13.36% |
| #4-15 | (-52,43) | 88.85 | 0.31% | 0.32% | 4.78% | -0.22% | -0.27% | 22.47% |
| | (-17,12) | 88.85 | 0.99% | 0.58% | 41.63% | -0.55% | -0.65% | 18.32% |

# 4. Conclusion

The impact resistance of PDC was studied by using DIT drop weight testing machine and DIC method. The results are as follows:

(1) The impact times of the anti-wear composite plate are less, the impact power is lower, and the final failure form is local delamination near the impact point edge.

(2) The impact resistant composite sheet has more total impact times and higher impact energy, and the final failure form is the overall breakage of polycrystalline layer of PDC composite sheet caused by crack propagation.

(3) PDC composite sheet is a brittle material, and the failure is the maximum tensile strain failure. According to the surface strain of the specimen, the strain concentration area on the surface of the PDC composite sheet will increase with the increase of impact times, and all of them are tensile strains.

(4) Using DIC to study images captured by high-speed cameras, the failure process of PDC composite films can be completely analyzed.

# References


[1] Zhang Fu xiao, Lu Yanjun, Xie Dou, Luo Hongbo, Shi Rui, Zhang Pei. Experimental study on the impact resistance of interface structure to PDC cutting tooth[J]. Engineering Failure Analysis, 2022, 140.

[2] Xi Yan, Wang Wei, Zha Chunqing, Li Jun Liu Gonghui. (2022). Numerical investigations on rock breaking mechanism and parameter influence of torsional percussive drilling with a single PDC cutter.Journal of Petroleum Science and Engineering.

[3] Zhiling Xiao, et al.Structural Design and Analysis of Large-Diameter D30 Conical Polycrystal Diamond Compact (PDC) Teeth under Engineering Rotary Mining Conditions.Materials 17.2(2024):.

[4] Li X ,Summers D ,Rupert G , et al.Experimental investigation on the breakage of hard rock by the PDC cutters with combined action modes[J].Tunnelling and Underground Space Technology incorporating Trenchless Technology Research, 2001, 16(2): 107-114.

[5] Wang, J.L.; Zhang, S.H.; Yang, K. Impact resistance of polycrystalline diamond compacts button insert using in DTH bit. Mater. Sci.Eng. Powder Metall. 2014, 19, 479–485.

[6] ZHANG Tao, Lu Canhua, Dou Ming et al. Development of diamond composite sheet for high performance oil drilling [J]. Superhard Materials Engineering, 2017, 29(03): 13-18.

[7] Sun Wei, ZHAO Haifeng, Zhang Tianxiang et al. Experimental study on improving impact resistance of diamond composite

sheet [J]. Drilling & Production Technology, 2018, 41(06): 87-89+105+10.

[8] Zhang Suhui, Wang Chuanliu, Dai Yongbo. Effect of temperature on performance of PDC cutters with different shapes [J]. Coal Geology and Exploration, 2020, 48(01): 240-245..

[9] Qi Xianyin, Wang Shengwei, Yang Zhen et al. Research on composite rock test and damage model based on digital image [J]. Science Technology and Engineering, 2022, 22(30): 13450-13459.

[10] Tung, S.H., Shih, M.H., Kuo, J.C. (2010). Application of digital image correlation for anisotropic plastic deformation during tension testing. Optics and Lasers in Eng., 48(5), 636−641.

[11] A.J. Comer,K.B. Katnam,W.F. Stanley,T.M. Young. Characterising the behaviour of composite single lap bonded joints using digital image correlation[J]. International Journal of Adhesion and Adhesives, 2013, 40.

[12] Sudarsanan N ,Arulrajah A ,Karpurapu R , et al. Digital Image Correlation Technique for Measurement of Surface Strains in Reinforced Asphalt Concrete Beams under Fatigue Loading[J]. Journal of Materials in Civil Engineering, 2019, 31(8).

[13] Mengying Liu,Ian McCue,Michael J. Demkowicz. Quantifying surface deformation around micrometer-scale indents by digital image correlation[J]. Journal of Materials Research, 2021(prepublish).

[14] R. P J ,Iyer R K ,Richard T , et al.DIC Based Strain and Damage Analysis of Large Scale Steel to Composite Adhesive Joints Subjected to Tension and Compression Loading[J].China Ocean Engineering,2023,37(4):588-597..

[15] Tao D ,Ping C ,Fei W , et al.Strain field evolution and crack coalescence mechanism of composite strength rock-like specimens with sawtooth interface[J].Theoretical and Applied Fracture Mechanics,2023,126.

[16] H. J H D V ,A. W S .The Effect of Specimen Thickness on the Lüders Phenomena in AISI 1524 Steel Alloy: Experimental Observations Using DIC[J].Experimental Mechanics, 2023, 63(5): 885-896.

[17] J. Blaber,B. Adair,A. Antoniou. Ncorr: Open-Source 2D Digital Image Correlation Matlab Software[J]. Experimental Mechanics, 2015, 55(6).

[18] Cheng Yuan-sheng. An approximate relation between compressive strength and tensile strength of some brittle materials—— a revision of the second strength theory [J]. Physical and chemical test. Physics Branch, 1981, 17(06): 30-31.